# Triple ionization chamber method for clinical dose monitoring with a Be-covered Li BNCT field

Thanh Tat Nguyen, Tsuyoshi Kajimoto, Kenichi Tanaka, Chien Cong Nguyen,[a)] and Satoru Endo[a),b)]
*Quantum Energy Applications, Graduate School of Engineering, Hiroshima University, 1-4-1 Kagamiyama, Higashi-Hiroshima, Hiroshima 739-8527, Japan*

(Received 9 December 2015; revised 6 September 2016; accepted for publication 10 September 2016; published 20 October 2016)

**Purpose:** Fast neutron, gamma-ray, and boron doses have different relative biological effectiveness (RBE). In boron neutron capture therapy (BNCT), the clinical dose is the total of these dose components multiplied by their RBE. Clinical dose monitoring is necessary for quality assurance of the irradiation profile; therefore, the fast neutron, gamma-ray, and boron doses should be separately monitored. To estimate these doses separately, and to monitor the boron dose without monitoring the thermal neutron fluence, the authors propose a triple ionization chamber method using graphite-walled carbon dioxide gas (C–$CO_2$), tissue-equivalent plastic-walled tissue-equivalent gas (TE-TE), and boron-loaded tissue-equivalent plastic-walled tissue-equivalent gas [TE(B)-TE] chambers. To use this method for dose monitoring for a neutron and gamma-ray field moderated by $D_2O$ from a Be-covered Li target (Be-covered Li BNCT field), the relative sensitivities of these ionization chambers are required. The relative sensitivities of the TE-TE, C–$CO_2$, and TE(B)-TE chambers to fast neutron, gamma-ray, and boron doses are calculated with the particle and heavy-ion transport code system (PHITS).
**Methods:** The relative sensitivity of the TE(B)-TE chamber is calculated with the same method as for the TE-TE and C–$CO_2$ chambers in the paired chamber method. In the Be-covered Li BNCT field, the relative sensitivities of the ionization chambers to fast neutron, gamma-ray, and boron doses are calculated from the kerma ratios, mass attenuation coefficient tissue-to-wall ratios, and $W$-values. The Be-covered Li BNCT field consists of neutrons and gamma-rays which are emitted from a Be-covered Li target, and this resultant field is simulated by using PHITS with the cross section library of ENDF-VII. The kerma ratios and mass attenuation coefficient tissue-to-wall ratios are determined from the energy spectra of neutrons and gamma-rays in the Be-covered Li BNCT field. The $W$-value is calculated from recoil charged particle spectra by the collision of neutrons and gamma-rays with the wall and gas materials of the ionization chambers in the gas cavities of TE-TE, C–$CO_2$, and TE(B)-TE chambers ($^{10}$B concentrations of 10, 50, and 100 ppm in the TE-wall).
**Results:** The calculated relative sensitivity of the C–$CO_2$ chamber to the fast neutron dose in the Be-covered Li BNCT field is 0.029, and those of the TE-TE and TE(B)-TE chambers are both equal to 0.965. The relative sensitivities of the C–$CO_2$, TE-TE, and TE(B)-TE chambers to the gamma-ray dose in the Be-covered Li BNCT field are all 1 within the 1% calculation uncertainty. The relative sensitivities of TE(B)-TE to boron dose with concentrations of 10, 50, and 100 ppm $^{10}$B are calculated to be 0.865 times the ratio of the in-tumor to in-chamber wall boron concentration.
**Conclusions:** The fast neutron, gamma-ray, and boron doses of a tumor in-air can be separately monitored by the triple ionization chamber method in the Be-covered Li BNCT field. The results show that these doses can be easily converted to the clinical dose with the depth correction factor in the body and the RBE.  [http://dx.doi.org/10.1118/1.4963222]

Key words: accelerator-based boron neutron capture therapy, triple ionization chamber method, neutron boron dose

## 1. INTRODUCTION

Fast neutron, gamma-ray, and boron doses have different relative biological effectiveness (RBE) of 3.2, 1, and 3.8, respectively.[1] In boron neutron capture therapy (BNCT), the clinical dose is the total of these dose components multiplied by their RBE. Clinical dose monitoring is necessary for quality assurance of the irradiation profile; therefore, the fast neutron, gamma-ray, and boron doses should be separately monitored.

In most BNCT facilities, the gamma-ray dose is monitored by using a thermoluminescence dosimeter.[2–4] The boron dose is monitored by the gold activation method with foils or wires, and the fast neutron dose is monitored by measuring the neutron fluence with a fission chamber. Rogus *et al.* used tissue-equivalent plastic-walled tissue-equivalent gas (TE-TE) and graphite-walled carbon dioxide gas (C–$CO_2$) chambers and the gold foil activation method to separate fast neutron, gamma-ray, and boron doses at the MITR-II research reactor.[5] However, the gold activation method takes 15 min to determine the thermal neutron fluence.[6] Recently, several simple methods have been proposed for dose monitoring. Ishikawa *et al.* proposed paired scintillator detectors with an optical fiber (SOF) system. The paired SOF consisted of boron-free and boron-loaded scintillator detectors to acquire the thermal neutron fluence quickly.[7] In addition, Becker *et al.* proposed a triple ionization chamber method with the TE-TE and magnesium-walled argon gas (Mg–Ar) chambers of the paired chamber method, and a Mg–Ar chamber coated with $^{10}$B on the inside surface of the chamber wall [Mg(B)–Ar].[8] The Mg(B)–Ar chamber with the $^{10}$B-coated Mg wall had a good response to the thermal neutrons. The boron dose was monitored by multiplying the kerma factor by the thermal neutron fluence which was determined by the Mg(B)–Ar chamber. Moreover, Fujii *et al.* investigated the optimization of the chamber wall thickness in a multionization-chamber system to improve the separation of thermal neutrons, epithermal neutrons, fast neutrons, and gamma-rays in BNCT.[9] They added a boron-loaded polyethylene-walled $N_2$ gas chamber and a silicon nitride-walled $N_2$ gas chamber to the paired chamber method in order to monitor the thermal and epithermal neutron fluences, respectively. In these methods, the boron dose was obtained from the measured thermal neutron fluence by multiplying by the kerma factor. Thus, a simple method is needed to estimate the boron dose without relying heavily on the determination of the thermal neutron fluence.

We propose a triple ionization chamber method to monitor the three dose components separately. This method uses the C–$CO_2$ and TE-TE chambers of the paired chamber method and a boron-loaded tissue-equivalent plastic-walled tissue-equivalent gas [TE(B)-TE] chamber. The TE(B)-TE chamber has the same constituents as the TE-TE chamber, except for small amount of $^{10}$B which is contained in TE wall. The paired chamber method with the TE-TE chamber and the C–$CO_2$ chamber have been used to determine the fast neutron dose and the gamma-ray dose.[10] The TE(B)-TE chamber is used to obtain the boron dose. The triple ionization chamber method with the TE-TE, C–$CO_2$, and TE(B)-TE chambers is an extension of the paired chamber method. To use our method for dose monitoring in a neutron and gamma-ray field moderated by $D_2O$ from a Be-covered Li target (Be-covered Li BNCT field), the relative sensitivities of three ionization chambers to fast neutron, gamma-ray, and boron doses are calculated with the particle and heavy-ion transport code system (PHITS)[11] with the cross section library of ENDF-VII.[12]

## 2. MATERIALS AND METHODS

### 2.A. Formulae for relative sensitivities of the triple ionization chamber method

The readings (unit: Gy) from the three chambers [TE-TE, $R_T$; C–$CO_2$, $R_U$; and TE(B)-TE, $R_B$] are expressed using the relative sensitivities of the ionization chambers of $k$, $h$, and $\alpha$ for the fast neutron, gamma-ray, and boron doses, respectively, as[10]

$$R_T = k_T D_N + h_T D_G, \tag{1}$$

$$R_U = k_U D_N + h_U D_G, \tag{2}$$

$$R_B = k_T D_N + h_T D_G + \alpha_B D_B, \tag{3}$$

where $D_N$, $D_G$, and $D_B$ are the fast neutron, gamma-ray, and boron doses (unit: Gy), respectively. Subscripts $T$, $U$, and $B$ indicate the TE-TE, C–$CO_2$, and TE(B)-TE chambers, respectively. Equations (1) and (2) are used for the paired chamber method.[10] The TE-TE and C–$CO_2$ chambers contain no $^{10}$B; therefore, they have no response to the boron dose which is originated in the $^{10}$B$(n,\alpha)^7$Li reaction. The triple ionization chamber method is based on the paired chamber method with an added TE(B)-TE chamber with a small amount of $^{10}$B in the wall. The reading as stated in Eq. (3) includes the fast neutron, gamma-ray doses of TE-TE chamber, and the boron dose. The relative sensitivity of the TE(B)-TE chamber to boron dose is $\alpha_B$, and those to fast neutron and gamma-ray doses are the same as $k_T$ and $h_T$ of the TE-TE chamber. With Eq. (3) the boron dose can be monitored separately by using the relative sensitivities of each chamber instead of multiplying the kerma factor by the thermal neutron fluence for this technique.

The relative sensitivities of the ionization chambers to the fast neutron and gamma-ray doses depend on the radiation field and are defined according to ICRU 26.[10] Zeeman *et al.* expressed these quantities of the ionization chambers with the following parameters: the $W$-value ratio of the $W$-value of the gamma-ray field from $^{60}$Co to that of the radiation field of interest, $W_C/W$ (definition of W value is described in Subsection 2.B.3 below); the wall-to-gas mass stopping power ratio, $S_{\mathrm{mg}}$; the mass-energy absorption coefficients tissue-to-wall ratio, $(\mu_{\mathrm{en}}/\rho)_t/(\mu_{\mathrm{en}}/\rho)_m$, where $S$, $\mu_{\mathrm{en}}$, and $\rho$ are mass stopping power, mass-energy absorption coefficient, and density of material, respectively; and the kerma tissue-to-gas ratio, $(K_t/K_g)$, as in Eqs. (4) and (5).[13] The relative sensitivity of the TE(B)-TE chamber to boron dose is similarly defined by Eq. (6),

$$k_{T,U} = \frac{W_C}{W_N}\left(S_{\mathrm{mg}}\right)_C \frac{((\mu_{\mathrm{en}}/\rho)_t/(\mu_{\mathrm{en}}/\rho)_m)_C}{\left(K_t/K_g\right)_N}, \tag{4}$$

$$h_{T,U} = \frac{W_C}{W_G}\frac{\left(S_{\mathrm{mg}}\right)_C}{\left(S_{\mathrm{mg}}\right)_G}\frac{((\mu_{\mathrm{en}}/\rho)_t/(\mu_{\mathrm{en}}/\rho)_m)_C}{((\mu_{\mathrm{en}}/\rho)_t/(\mu_{\mathrm{en}}/\rho)_m)_G}, \tag{5}$$

$$\alpha_B = \frac{W_C}{W_B}\frac{\left(S_{\mathrm{mg}}\right)_C}{\left(S_{\mathrm{mg}}\right)_B}\frac{((\mu_{\mathrm{en}}/\rho)_t/(\mu_{\mathrm{en}}/\rho)_m)_C}{(K_t/K_m)_B}. \tag{6}$$

Here, subscripts $t$, $m$, $g$, $C$, $N$, $G$, and $B$ denote tissue, wall material, gas, reference gamma-ray dose (e.g., $^{60}$Co gamma-rays), fast neutron, gamma-ray, and boron doses,

TABLE I. $W$-values, mass attenuation coefficient tissue-to-wall ratios, and wall-to-gas mass stopping power ratios of the TE-TE and C–$CO_2$ chambers in the $^{60}$Co gamma-ray field.

| Symbol | Ionization chamber | Value | Reference |
|---|---|---|---|
| $W_C$ | TE-TE | 29.3 eV | 14 |
| | C–$CO_2$ | 33.0 eV | 17 |
| $((\mu_{en}/\rho)_t/(\mu_{en}/\rho)_m)_C$ | TE-TE | 1.001 | 14 |
| | C–$CO_2$ | 1.126 | 16 |
| $(S_{mg})_C$ | TE-TE | 1.000 | 14 |
| | C–$CO_2$ | 1.009 | 15 |

respectively. $W_N$, $W_B$,$(S_{mg})_B$, and $W_G$ are calculated based on the recoil particle energy spectra in the gas cavity of ionization chambers, and $(K_t/K_g)_N$ and $((\mu_{en}/\rho)_t/(\mu_{en}/\rho)_m)_G$ are calculated from the neutron and gamma-ray energy spectra. The parameters of $W_C$, $(S_{mg})_C$, and $((\mu_{en}/\rho)_t/(\mu_{en}/\rho)_m)_C$ for the $^{60}$Co gamma-ray field are taken from the literature and are listed in Table I.[14–17] The calculation method for the $W$-value, kerma ratio, mass energy absorption coefficient tissue-to-wall ratio, and wall-to-gas mass stopping power ratio is described in Subsection 2.B.

In order to use the triple ionization chamber method for dose monitoring, we are planning for the three-monitor chamber to be set at the surface of the treatment position. The dose components are monitored as the tumor kerma in-air. For boron dose monitoring, when the $^{10}$B concentration in tissue is assumed to be that in the tumor, $\rho_t$, the $^{10}$B concentration in the chamber wall is $\rho_c$, the ratio of kerma in tissue to kerma in the TE(B)-TE chamber wall from $\alpha$ particles and Li ions produced: $(K_t/K_m)_B$ corresponds to $\rho_t/\rho_c$. Therefore, $\alpha_B$ in Eq. (6) can be expressed by $\alpha'_B$ as

$$\alpha_B = \frac{\rho_c}{\rho_t}\alpha'_B, \tag{7}$$

$$\alpha'_B = \frac{\overline{W_c}}{W_B}\frac{(S_{mg})_C}{(S_{mg})_B}((\mu_{en}/\rho)_t/(\mu_{en}/\rho)_m)_C, \tag{8}$$

where reduced relative sensitivity $\alpha'_B$ is not dependent on the $^{10}$B concentration in the wall of the TE(B)-TE chamber. The parameters for calculating the TE(B)-TE chamber are assumed to be the same as those of the TE-TE chamber because of the negligible $^{10}$B content of 10, 50, or 100 ppm. To estimate the tumor dose in the body, a correction factor dependent on the depth from the surface is needed. This correction factor is discussed in Sec. 4.

## 2.B. Relative sensitivity calculations

### 2.B.1. Calculation of neutron and gamma-ray energy spectra

Neutrons that are produced by the $^7$Li($p$,$n$) reaction from a Be-covered Li target are considered as the neutron source for this study. The cross section of the $^7$Li($p$,$n$)$^7$Be reaction in the proton reaction sublibrary of ENDF-VII (Ref. 12) is used to estimate the source term by PHITS. The target consists of a Li layer (100 $\mu$m thick, 12 cm in diameter) covered with a Be layer (20 $\mu$m thick). The Be-covered Li target is attached on a Cu backing plate (0.8 cm thick, 14 cm in diameter), target assembly (SUS304 stainless steel, 1.4 cm thick), and circulating cooling water (2.2 cm effective thickness). In this calculation, the incident proton beam from the accelerator is assumed with the current, section diameter, and energy to be 1 mA, 10 cm, and 2.86 MeV, respectively. Due to the existence of Be layer on the surface of Li target, the proton energy is reduced to 2.5 MeV at the surface of the Li layer. To save calculation time, the calculation of the neutron energy spectrum at the collimator exit is divided into two steps. First, the proton-induced neutron energy spectrum from the target is tallied at the downstream surface of the Li target. Second, generated neutrons from the downstream surface of the target are transported through the Cu backing plate, cooling water, target assembly, $D_2O$ moderator (20 cm thickness and 20 cm in diameter), and a collimator (polyethylene + 50 wt. % natural LiF, 12 cm inside diameter, and a 10 cm outside diameter). This neutron energy spectrum is tallied at the collimator exit. The simulation geometry is shown in Fig. 1, and the neutron energy spectrum is shown in Fig. 2.

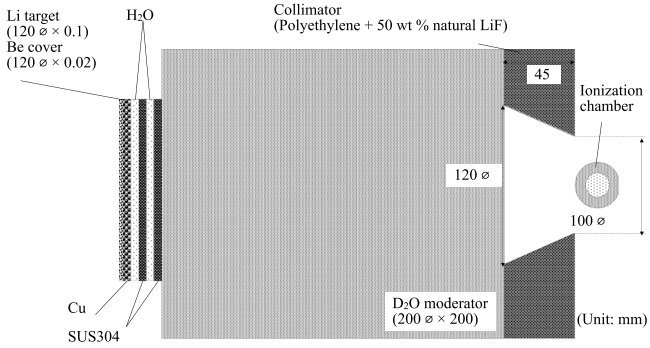


FIG. 1. Input geometry for the PHITS calculations.

Gamma-rays are produced by the $^7$Li($p$,$p'\gamma$) reaction (prompt gamma-rays: PG) and by interaction between neutron and materials around the target, such as Cu, $H_2O$, SUS304

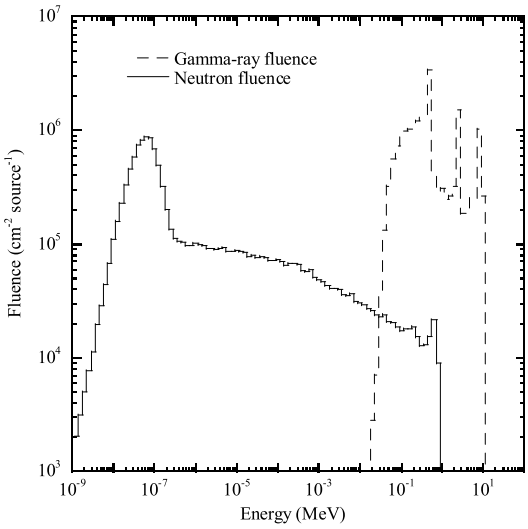


FIG. 2. Neutron and gamma-ray spectra at the collimator exit.

(secondary gamma-rays: SG). However, owing to the lack of cross section data for $^{7}$Li($p$,$p'\gamma$) reaction in the cross section library ENDF-VII, the prompt gamma-rays with an energy of 478 keV from the ($p$,$p'\gamma$) reaction are produced from an isotropic point source at the center of the Li target according to Lee's method,[18] and they are transported through the cooling system, moderator, and collimator. The other gamma-ray production such as the $^{7}$Li($p$,$\gamma$) reaction, gamma-ray from the first excited state through the $^{7}$Li($p$,$n$)$^{7}$Be$^{*}$ reaction, and decay gamma-rays from the resultant $^{7}$Be by the $^{7}$Li($p$,$n$)$^{7}$Be reaction, are negligibly small (less than 2% of the total of PG and SG at the collimator exit). The total gamma-ray spectra are shown at the exit of the collimator in Fig. 2. These spectra are used for further chamber simulations.

### 2.B.2. Recoil particle spectra in ionization chamber gas cavities

The recoil particle spectra produced in the gas cavity of each chamber in the Be-covered Li BNCT field are calculated with neutron and gamma-ray spectra from Fig. 2 by PHITS. These spectra are used for calculating the $W$-values. The input geometries of the TE-TE, C–$CO_2$, and TE(B)-TE chambers are assumed to be spherical (IC-17, Farwest Technology Co. Ltd.). The C–$CO_2$ ionization chamber has graphite walls (543 mg cm$^{-2}$), an internal volume of 2.5 cm$^3$, and is filled with $CO_2$ gas. The TE-TE chamber has a TE wall (A-150 wall) (569 mg cm$^{-2}$), an internal volume of 1 cm$^3$, and is filled with methane-based TE gas. The TE(B)-TE has the same geometry as the TE-TE chamber except for a small amount of $^{10}$B (10, 50, or 100 ppm) in the TE wall.

The element compositions of TE-TE, C–$CO_2$, and TE(B)-TE chambers[19] are summarized in Table II. Each ionization chamber is set at the collimator exit in this calculation, as shown in Fig. 1.

### 2.B.3. W-value calculation

The $W$-value is the ratio of the total deposited energy to the total number of electron-ion pairs in the gas cavity produced by incident neutron or gamma-ray in the ionization chamber. For fast neutrons, the energy deposition and ion pairs are from H, C, O, and N ions, similar to $\alpha$ particles and Li ions produced by the $^{10}$B($n$,$\alpha$)$^{7}$Li reaction. For gamma-rays, the energy deposition and ion pairs originate from electrons emitted from the walls and gas by ionization and electron-position pair production processes. In this calculation, the $W$-values for fast neutrons ($W_N$), gamma-rays ($W_G$), and the sum of $\alpha$ particles and Li ions ($W_B$) is calculated from the initial differential energy spectrum, $n_j(E_i)$, for recoil charged particles of type $j$, in the gas cavity of ionization chambers. The average energies per ion pair of $W_N$, $W_G$, and $W_B$ are obtained as

$$W = \frac{\sum_j \sum_i n_j(E_i) E_i \Delta E_i}{\sum_j \sum_i n_j(E_i) E_i \Delta E_i / W_j(E_i)}, \tag{9}$$

where $W_j(E_i)$ is the $j$th recoil particle $W$-value at the $i$th energy group, $E_i$. Summation over $j$ is carried out by H, C, N, and O ions for fast neutrons, electrons for gamma-rays, and $\alpha$ particles and Li ions induced by the $^{10}$B($n$,$\alpha$)$^{7}$Li reaction, which is related to the boron dose. $W_j(E_i)$ ($j$ = H, $\alpha$, C, N, O) in TE gas are taken from the values reported by Goodman and Coyne.[20] $W_{\mathrm{Li}}(E)$ of Li ion in TE gas is calculated using the scaling law from $W_\alpha(E)$ of $\alpha$ particles with the corresponding reduced energy $\varepsilon = E/Mz^{4/3}$, where $M$ is the particle mass and $z$ is the nuclear charge.[17] $W_j(E_i)$ for $j$ = H, $\alpha$, Li, C, N,

TABLE II. Compositions of TE-TE, C–$CO_2$, and TE(B)-TE chambers.

| | Composition (%) | | | | |
|---|---|---|---|---|---|
| Element | TE wall | TE(B) wall | Methane-based TE gas | C wall | $CO_2$ gas |
| H | 10.1 | 10.1 | 10.2 | — | — |
| C | 77.7 | 77.7 | 45.6 | 100 | 27.3 |
| N | 3.5 | 3.5 | 3.5 | — | — |
| O | 5.2 | 5.2 | 40.7 | — | 72.7 |
| F | 1.7 | 1.7 | — | — | — |
| Ca | 1.8 | 1.8 | — | — | — |
| B | — | 10, 50, 100 ppm $^{10}$B | — | — | — |

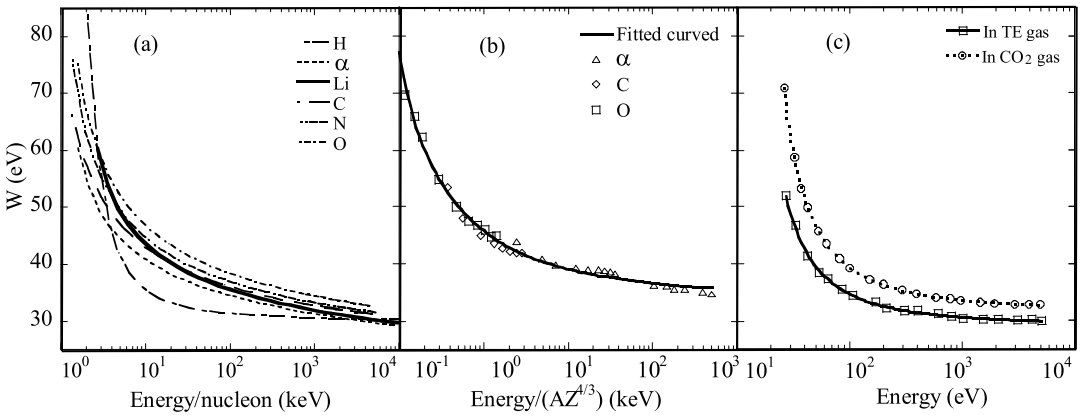


FIG. 3. (a) Average energy per ion pair of $\alpha$ particles, and H, Li, C, N, and O ions in TE gas (Ref. 20). (b) Fitted curve of the average energy per ion pair of $\alpha$ particles and C and O ions in $CO_2$ gas (Ref. 21). (c) Fitted curve of the average energy per ion pair of electrons in TE and $CO_2$ gases (Refs. 17 and 21).

TABLE III. Fitting parameters of Eqs. (10) and (11).

| | $a$ | $b$ | $c$ | $d$ |
|---|---|---|---|---|
| $\alpha$ particles and C and O ions in $CO_2$ gas | 12.22 | 0.94 | 0.35 | 27.04 |
| Electrons in TE gas | 995.24 | 7.25 | 3.47 | 29.32 |
| Electrons in $CO_2$ gas | 1396.3 | 9.5 | 3.49 | 31.89 |

O in TE gas are shown in Fig. 3(a). Several experimental values for $W_j(E_i)$ ($j = \alpha$, C, O) in $CO_2$ gas are available at energies of $24.5\times10^3$ to $5.11\times10^3$ keV for $\alpha$ particles, and 24.5–370 keV for C and O ions.[21] Therefore, for $W_j(E_i)$ in $CO_2$ gas for $\alpha$ particles, C and O ions are obtained by a scaling function of $W(\varepsilon)$ with the reduced energy fitted using Eq. (10) [Fig. 3(b)]. $W_e(E_i)$ of electrons in TE and $CO_2$ gas are obtained by fitting with Eq. (11) based on previous data[17,21] [Fig. 3(c)]. The results of the fitted parameters are listed in Table III. The error of the fitted values and experimental values is less than 1% for electrons in TE/$CO_2$ gas and less than 3% for recoil particles in $CO_2$ gas,

$$W(\varepsilon) = \frac{a}{(0.434\ln(\varepsilon - b))^c} + d, \tag{10}$$

$$W_e(E) = \frac{a}{(\ln(E-b))^c} + d. \tag{11}$$

#### 2.B.4. Kerma ratio and mass-energy absorption coefficient tissue-to-wall ratio calculation

The kerma ratio of tissue-to-TE/$CO_2$ gas, $(K_t/K_g)_N$ for neutrons and the tissue-to-wall ratio of mass-energy absorption coefficients in tissue and the C/TE wall for gamma-rays are calculated as

$$(K_t/K_g)_N = \frac{\sum_i K_{f,t}(E_i)\Phi_n(E_i)}{\sum_i K_{f,g}(E_i)\Phi_n(E_i)}, \tag{12}$$

$$((\mu_{en}/\rho)_t/(\mu_{en}/\rho)_m)_G = \frac{\sum_i \left(\frac{\mu_{en}}{\rho}(E_i)\right)_t E_i\Phi_G(E_i)}{\sum_i \left(\frac{\mu_{en}}{\rho}(E_i)\right)_m E_i\Phi_G(E_i)}, \tag{13}$$

where subscripts $t$ and $g$ denote tissue and gas, respectively; $K_{f,t}(E_i)$ and $K_{f,g}(E_i)$ are kerma factors in tissue and TE/$CO_2$ gas at energy $E_i$ from the literature data,[19] respectively; the mass-energy absorption coefficients for each element are taken from the data reported by Hubbell and Seltzer;[22] and $\Phi_n(E_i)$ and $\Phi_G(E_i)$ are the neutron fluence and gamma-ray fluence at energy $E_i$, respectively. These neutron and gamma-ray fluences are obtained at the collimator exit.

#### 2.B.5. Wall-to-gas mass stopping power ratio calculation

The wall-to-gas mass stopping power ratio, $(S_{mg})_B$ for the Be–Li BNCT field is estimated from the mass stopping power of $\alpha$ particles and Li ions in the TE wall and TE gas according to the Bethe-Bloch formula[23] with the mean energy for $\alpha$ particles and Li ions. The $\alpha$ particle and Li ion energy spectra in TE wall and TE gas are calculated from the neutron fluence of the outputs in the second calculation step by PHITS.

## 3. RESULTS

### 3.A. *W*-value calculation from the recoil particle spectra in gas cavities

The recoil particle spectra induced by neutrons in the gas cavities of TE-TE, TE(B)-TE, and C–$CO_2$ chambers are shown in Figs. 4(a)–4(c). The electron spectra due to gamma-rays are shown in Fig. 4(d). Figure 4(a) shows the spectra of H, C, N, and O ions in the TE gas of TE-TE chamber. Figure 4(b) shows the identical spectra of H, C, N, and O ions with those in Fig. 4(a), and the energy spectra of $\alpha$ particles and Li ions for a $^{10}$B concentration of 100 ppm originating from the $^{10}B(n,\alpha)^7Li$ reaction in the boron-loaded TE-plastic [TE(B)-plastic] wall. The shape of energy spectra of $\alpha$ particles and Li ions does not change with the $^{10}$B concentration even in cases of 10 and 50 ppm [not shown in Fig. 4(b)] because $\alpha$ particle and Li ion yields are proportional to the $^{10}$B concentration. Therefore, at higher $^{10}$B concentrations in the TE(B)-TE chamber wall, the fraction of energy deposition and ion-pairs produced by $\alpha$ particles and Li ions increase. Figure 4(c) shows the spectra of C and O ions, which are products of neutron elastic scattering with C and O in the C–$CO_2$ chamber. A small amount of $\alpha$ particles is produced by the $^{17}O(n,\alpha)$ reaction, with a fluence of three orders of magnitude lower than C and O ions; therefore, its contribution to the $W_N$-value of the C–$CO_2$ chamber is negligible. Figure 4(d) shows the energy spectra of electrons in the TE gas of the TE-TE/TE(B)-TE chambers and $CO_2$ gas of the C–$CO_2$ chamber. Because the electrons from gamma-rays produced by the $^{10}B(n,\alpha\gamma)$ reaction are negligibly small (less than 0.1% compared to the electrons due to PG and SG), the energy spectra of electrons in the TE(B)-TE chamber do not change with the $^{10}$B concentration and are the same as that of the TE-TE chamber.

$W_N$ and $W_G$ for TE-TE, C–$CO_2$, and TE(B)-TE chambers, and $W_B$ for TE(B)-TE chamber are calculated, and the results are summarized in Table IV. The $W_N$ and $W_G$ for TE-TE chamber have the same values as those for TE(B)-TE chamber. The $W_B$ of the TE(B)-TE chamber is not dependent on $^{10}$B concentration.

### 3.B. Kerma ratio, mass-energy absorption coefficient tissue-to-wall ratio, and wall-to-gas mass stopping power ratio

The calculated results of the kerma ratios of the TE-TE, C–$CO_2$, and TE(B)-TE chambers, and the mass-energy absorption coefficient tissue-to-wall ratios are listed in Table IV. The wall-to-gas mass stopping power ratio is calculated by using the energy spectra of $\alpha$ particles and Li ions in Fig. 4(b).

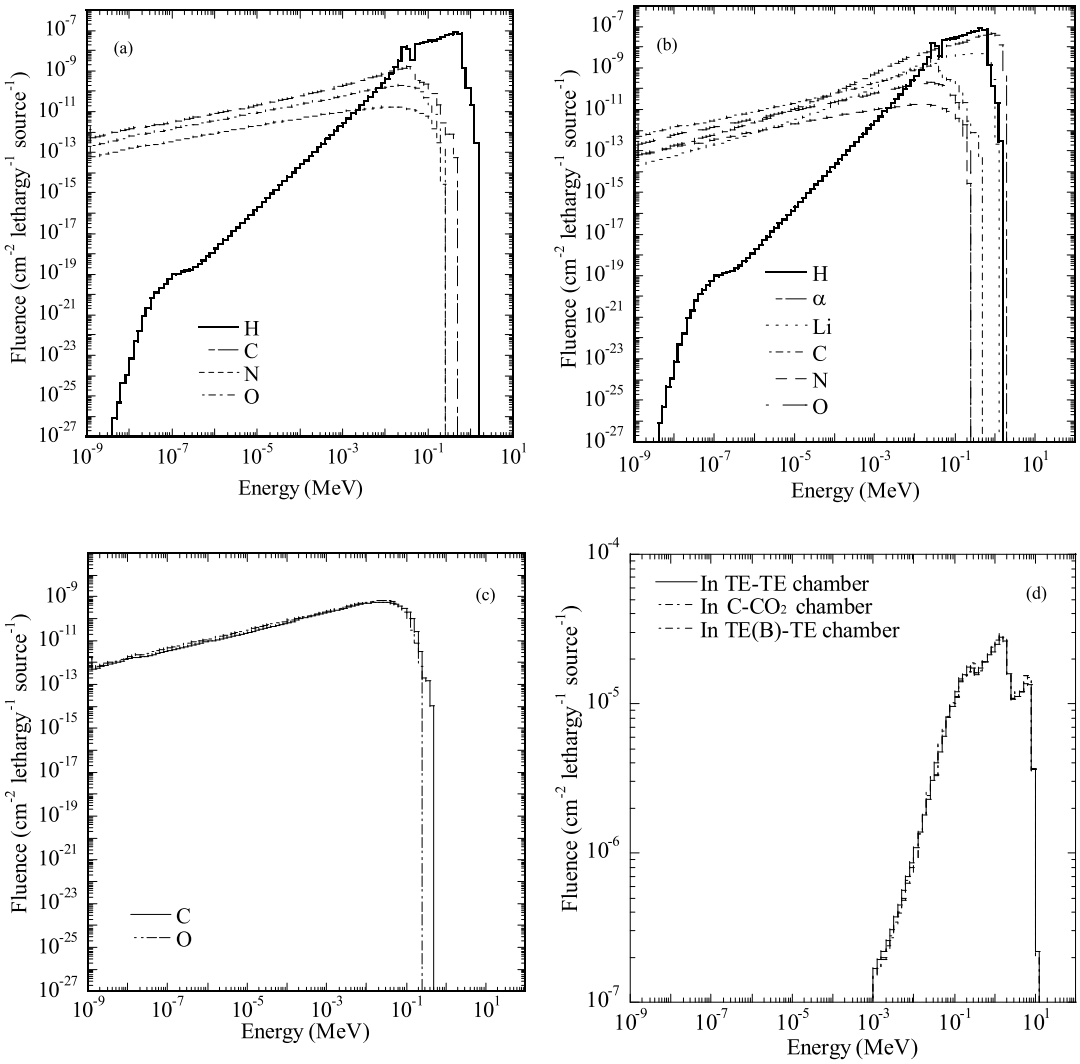


FIG. 4. (a) Recoil particle spectra in the TE gas in the TE-TE chamber. (b) Recoil particle spectra in the TE gas of the TE(B)-TE chamber at a $^{10}$B concentration of 100 ppm. (c) Recoil particle spectra in the $CO_2$ gas of the C–$CO_2$ chamber. (d) Electron spectra in the gas cavity of the TE-TE, C–$CO_2$, and TE(B)-TE chambers.

### 3.C. Relative sensitivities of ionization chambers

The relative sensitivities of the ionization chambers for the Be-covered Li BNCT field are listed in Table V. The relative sensitivities of the TE-TE and TE(B)-TE chambers to the fast neutron dose ($k_T$ and $k_B$) are the same; that of C–$CO_2$ chamber to the fast neutron dose, $k_U$ is approximately 33 times smaller than the $k_T$ and $k_B$ due to lack of hydrogen in chamber; and those of TE-TE, C–$CO_2$, and TE(B)-TE ($h_T$ and $h_U$) to the gamma-ray dose are 1 with the calculation uncertainty of 1%.

TABLE IV. Calculated results of the $W$-values, kerma ratios, mass attenuation coefficient tissue-to-wall ratios, and wall-to-gas mass stopping power ratio for the TE-TE, C–$CO_2$, and TE(B)-TE chambers.

| Symbol | Ionization chamber | Value |
|---|---|---|
| $W_N$ | TE-TE, TE(B)-TE | 30.82 eV |
| | C–$CO_2$ | 62.02 eV |
| $W_G$ | TE-TE, TE(B)-TE | 29.3 eV |
| | C–$CO_2$ | 33.0 eV |
| $W_B$ | TE(B)-TE | 33.8 eV |
| $(K_t/K_g)_N$ | TE-TE, TE(B)-TE | 0.986 |
| | C–$CO_2$ | 20.3 |
| $((\mu_{en}/\rho)_t/(\mu_{en}/\rho)_m)_G$ | C–$CO_2$ | 1.108 |
| $(S_{mg})_B$ | TE(B)-TE | 1.002 |

TABLE V. Relative sensitivities of the ionization chambers to the Be-covered Li BNCT field.

| | | Relative sensitivity | | |
|---|---|---|---|---|
| Chamber | Subscription | $k$ | $h$ | $\alpha'_B$ |
| C–$CO_2$ | $U$ | 0.029 | 1.000 | — |
| TE-TE | $T$ | 0.965 | 0.999 | — |
| TE(B)-TE | $B$ | 0.965 | 0.999 | 0.865[a] |
| | | | | 0.864[b] |
| | | | | 0.866[c] |

[a]10 ppm $^{10}$B.
[b]50 ppm $^{10}$B.
[c]100 ppm $^{10}$B.

The reduced relative sensitivity of the TE(B)-TE chamber to the boron dose, $\alpha'_B$ is independent of the $^{10}$B concentration in the chamber wall, as in Eq. (8). The calculated results of $\alpha'_B$ show the same value of 0.865 within the uncertainty of 5%.

The relative sensitivity of the TE(B)-TE chamber to boron dose, $\alpha_B$, is calculated as in Eq. (7). $\alpha_B$ depends on the ratio of the in-tumor ($\rho_t$) to TE(B)-TE chamber in-wall ($\rho_c$) $^{10}$B concentrations, and it is expressed as $0.865(\rho_c/\rho_t)$.

The uncertainties of the relative sensitivities to fast neutron and boron doses are estimated to be less than 5% for the fast neutron and boron doses and less than 1% for the gamma-ray dose with the PHITS statistical error calculation, and errors of other quantities in Refs. 20 and 24–26.

## 4. DISCUSSION

From the neutron and gamma-ray energy spectra in Fig. 2, the mean neutron energy weighted with the kerma factor is calculated to be 0.2 MeV and the mean gamma-ray energy weighted by the mass attenuation coefficient of gamma-rays is calculated to be 1.36 MeV. The relative sensitivities of TE-TE, C–$CO_2$, and TE(B)-TE chambers to gamma-ray, $h_T$ and $h_U$, are equal to unity within the calculation uncertainty. The calculated results of $h_T$ and $h_U$ are consistent with the recommended value of ICRU 26.[10] The relative sensitivities of the TE-TE chamber ($k_T$) and C–$CO_2$ chamber ($k_U$) to the fast neutron dose in the Be-covered Li BNCT field are plotted against the mean neutron energy [Figs. 5(a) and 5(b)] comparing with those for monoenergetic neutrons. The differences of $k_T$ in the Be-covered Li BNCT field and the results of Jansen *et al.* and Endo *et al.* for monoenergetic neutrons are 4.8% and 2.4%, respectively.[27,28] These differences are consistent with our calculation uncertainties. The $k_U$ value of our calculation has around 28% of difference from the calculation by Endo *et al.*[30] This difference seems large, however, propagated uncertainties of neutron and gamma-ray absorbed doses are not large as they are estimated to be around 5% and 1%, respectively. Therefore, the obtained relative sensitivities can be used for dose monitoring with sufficient uncertainty.

Based on the calculation results and Eqs. (1)–(3), the fast neutron, gamma-ray, and boron doses in the Be-covered Li BNCT field are expressed separately as

$$D_N = 1.1(R_T - R_U), \tag{14}$$

$$D_G = R_U - 0.03R_T, \tag{15}$$

$$D_B = 1.16\frac{\rho_t}{\rho_c}(R_B - R_T). \tag{16}$$

Monitored doses $D_N$, $D_G$, and $D_B$ are the tumor doses in-air. This shows that the boron dose can be monitored as $D_B$ in-air without considering the thermal neutron fluence if the $^{10}$B concentration in the tumor is known.

The tumor dose of the fast neutron, gamma-ray, and boron doses in the body should be corrected by the corresponding depth correction factor and the RBE. The RBE of these dose components can be taken from the IAEA-TECDOC 1223.[1] The total clinical dose, $D_C$ (Gy-Eq), in the tumor is calculated as

$$D_C = 3.2\eta_N \cdot D_N + \eta_G \cdot D_G + 3.8\eta_B \cdot D_B, \tag{17}$$

where subscripts $N$, $G$, and $B$ indicate fast neutron, gamma-ray, and boron doses, respectively, and $\eta_k$ ($k = N$, $G$, and $B$) is the depth correction factor for each dose component.

The $\eta_k$ is calculated by the ratio of the dose at each depth to that on the surface of the phantom. This ratio shows that a dose changes according to the spectrum distortion of neutrons

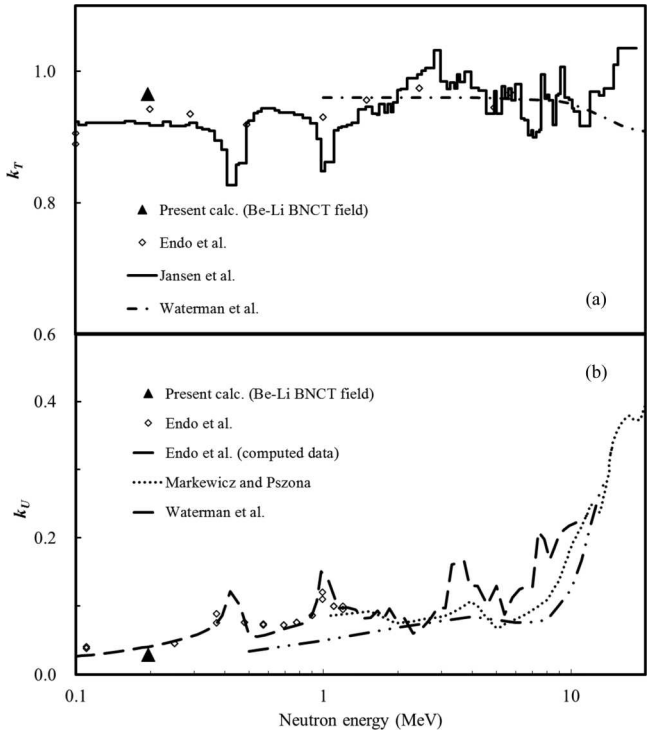


FIG. 5. (a) Calculated $k_T$ of the BNCT neutron field plotted against the mean neutron energy (closed triangles). Previous data for monoenergetic neutrons are shown for Refs. 27–29. (b) Calculated $k_U$ of the BNCT neutron field plotted against the mean neutron energy (closed triangles). Previous data for monoenergetic neutrons are shown for Refs. 29–31.

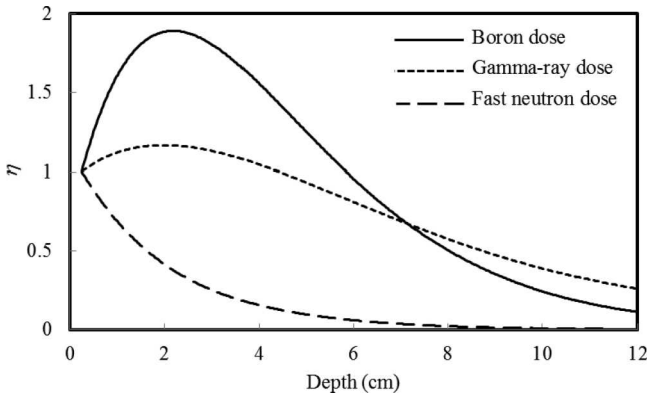


FIG. 6. Depth correction factor of fast neutron, gamma-ray, and boron doses.

and gamma-rays in the body. Tanaka *et al.*[32] calculated the depth dose curves in a light water phantom for fast neutron, gamma-ray, and boron doses for $D_2O$ moderated $^7Li(p,n)^7Be$ neutrons with 2.5 MeV incident protons. $\eta$ of the fast neutron, gamma-ray, and boron doses can be estimated from the depth dose curves (Fig. 6). In this research, these depth correction factors can be used to estimate the tumor doses in the body. The total clinical dose, $D_C$ (Gy-Eq), can be quickly calculated with Eq. (17). Thus, these doses can be converted easily to the clinical dose with the depth correction factor in the body and the RBE.

## 5. CONCLUSION

We proposed a triple ionization chamber method to monitor fast neutron, gamma-ray, and boron doses for BNCT. For the triple ionization chamber method, the relative sensitivities of the TE-TE, C–$CO_2$, and TE(B)-TE chambers in the neutron and gamma-ray field moderated by $D_2O$ from a Be-covered Li target were calculated. The fast neutron dose, gamma-ray dose, and boron dose of a tumor in-air were estimated by this method. The tumor dose in-air was converted to a clinical dose by correcting with the depth correction factor in the body and RBE. The results indicate that the clinical dose can be monitored by the triple ionization chamber method. The differences of $k_T$ at mean energy in the Be-covered Li BNCT field to monoenergetic neutrons are consistent with previous calculations within the calculation uncertainties. The $k_U$ is quite different from previous calculations, however, the uncertainties of neutron and gamma-ray absorbed doses are estimated to be around 5% and 1%, respectively.

## ACKNOWLEDGMENT

The authors are grateful to Asia Jinzai Program and Phoenix Leader Education Program of Hiroshima University for their financial support and good advice on writing a scientific paper.

## CONFLICT OF INTEREST DISCLOSURE

The authors have no COI to report.

[a]Present address: Engineering Department, Industrial Equipment Division, Sumitomo Heavy Industries, Ltd.
[b]Author to whom correspondence should be addressed. Electronic mail: endos@hiroshima-u.ac.jp

[1]IAEA, "Current status of neutron capture therapy," IAEA-TECDOC-1223 (IAEA, Vienna, 2001).
[2]C. Aschan, M. Toivonen, S. Savolainen, and F. Stecher-Rasmussen, "Experimental correction for thermal neutron sensitivity of gamma ray TL dosimeters irradiated at BNCT beams," Radiat. Prot. Dosim. **82**(1), 65–69 (1999).
[3]K. Tanaka, T. Kobayashi, Y. Sakurai, Y. Nakagawa, S. Endo, and M. Hoshi, "Dose distributions in a human head phantom for neutron capture therapy using moderated neutrons from 2.5 MeV proton-$^7$Li reaction or from fission of $^{235}$U," Phys. Med. Biol. **46**, 2681–2695 (2001).
[4]H. Joensuu *et al.*, "Boron neutron capture therapy of brain tumors: Clinical trials at the finnish facility using boronophenylalanine," J. Neuro-Oncol. **62**, 123–134 (2003).
[5]R. D. Rogus, O. K. Harling, and J. C. Yanch, "Mixed field dosimetry of epithermal neutron beams for boron neutron capture therapy at the MITR-II research reactor," Med. Phys. **21**, 1611–1625 (1994).
[6]M. Ishikawa *et al.*, "A statistical estimation method for counting of the prompt gamma-rays from $^{10}B(n,\alpha\gamma)^7Li$ reaction by analyzing the energy spectrum," Nucl. Instrum. Methods Phys. Res., Sect. A **453**, 614–620 (2000).
[7]M. Ishikawa, K. Ono, Y. Sakurai, H. Unesaki, A. Uritani, G. Bengua, T. Kobayashi, K. Tanaka, and T. Kosako, "Development of real-time thermal neutron monitor using boron-loaded plastic scintillator with optical fiber for boron neutron capture therapy," Appl. Radiat. Isot. **61**, 775–779 (2004).
[8]J. Becker, E. Brunckhorst, A. Roca, F. Stecher-Rasmussen, R. Moss, R. Bottger, and R. Schmidt, "Set-up and calibration of a triple ionization chamber system for dosimetry in mixed neutron/photon fields," Phys. Med. Biol. **52**(13), 3715–3727 (2007).
[9]T. Fujii, H. Tanaka, A. Maruhashi, K. Ono, and Y. Sakurai, "Study on optimization of multiionization-chamber system for BNCT," Appl. Radiat. Isot. **69**, 1862–1865 (2011).
[10]International Commission on Radiation Units (ICRU), "Neturon dosimetry for biology and medicine," ICRU Report 26 (ICRU, Washington, DC, 1977).
[11]H. Iwase, K. Niita, and T. Nakamura, "Development of general purpose particle and heavy ion transport Monte Carlo code," J. Nucl. Sci. Technol. **39**, 1142–1151 (2002).
[12]M. B. Chadwick *et al.*, "ENDF/B-VII.1 Nuclear data for science and technology: Cross sections, covariances, fission product yields and decay data," Nucl. Data Sheets **112**, 2887–2996 (2011).
[13]G. H. Zeeman and K. P. Ferlic, "Paired ion chamber constants for fission gamma-neutron field," Technical Report TR84–8 (Armed Forces Radiobiology Research Institute, Washington, DC, 1984).
[14]J. J. Broerse, B. J. Mijnheer, and J. R. Williams, "European protocol for neutron dosimetry for external beam therapy," Br. J. Radiol. **54**, 882–898 (1981).
[15]AAPM, "Protocol for neutron beam dosimetry," AAPM Report No. 7 (American Association of Physicists in Medicine, American Institute of Physics, New York, NY, 1980).
[16]DLC-31/(DPL-1/FEWG1), "37-neutron, 21-gamma ray coupled, P3, multigroup library in ANISN format," ORNL/TM-4840, Oak Ridge National Laboratories, Oak Ridge, TN, 1975.
[17]International Commission on Radiation Units and Measurement (ICRU), "Average energy required to produce an ion pair," ICRU Report 31 (ICRU, Washington, DC, 1979).
[18]C. L. Lee, X. L. Zhou, R. J. Kudchadker, F. Harmon, and Y. D. Harker, "A Monte Carlo dosimetry-based evaluation of the $^7Li(p,n)^7Be$ reaction near threshold for accelerator boron neutron capture therapy," Med. Phys. **27**, 192–202 (2000).
[19]International Commission on Radiation Units (ICRU), "Tissue substitutes in radiation dosimetry and measurement," ICRU Report 44 (ICRU, Washington, DC, 1979).
[20]L. J. Goodman and J. J. Coyne, "Wn and neutron kerma for methane-based tissue-equivalent gas," Radiat. Res. **82**, 13–26 (1982).
[21]IAEA, "Atomic and molecular data for radiotherapy and radiation research," IAEA-TECDOC-799 (IAEA, Vienna, 1995).
[22]J. H. Hubbell and S. M. Seltzer, "Tables of X-ray mass attenuation coefficients and mass energy-absorption coefficients from 1 keV to 20 MeV for elements z = 1 to 92 and 46 additional substances of dosimetric interest," in *NIST Standarad Reference Database 126* (National Institute of Standards and Technology, U.S. Department of Commerce, 2004).
[23]H. A. Bethe and J. Ashkin, in *Experimental Nuclear Physics, Part II*, edited by E. Segre (John Wiley and Sons, Inc., New York, NY, 1953), p. 116.
[24]V. D. Nguyen, M. Chemtob, J. Chary, F. Posny, and N. Parmentier, "Recent experimental results on W values for heavy particles," Phys. Med. Biol. **25**(3), 509–518 (1980).
[25]B. G. R. Smith and J. Booz, "Experimental results on W-Values and transmission of low energy electron gases," in *Proceedings of the Sixth Symposium on Microdosimetry, Report No. Eur-6064* (Harwood Academic Publisher, Ltd., London, 1978), p. 759.
[26]International Commission on Radiation Units (ICRU), "Photon, electron, proton and neutron interaction data for body tissues," ICRU Report 46 (ICRU, Bethesda, MD, 1992).

[27]S. Endo, M. Hoshi, K. Shizuma, J. Takada, and D. T. Goodhead, "Calculation of the neutron W value for neutron dosimetry below the MeV energy region," Phys. Med. Biol. **45**, 947–953 (2000).
[28]J. T. M. Jansen, C. P. J. Raaijmakers, B. J. Mijheer, and J. Zoetelief, "Relative neutron sensitivity of tissue equivalent ionization chambers in an epithermal neutron," Radiat. Prot. Dosim. **70**, 27–32 (1997).
[29]F. M. Waterman, F. T. Kuchinir, L. S. Skaggs, R. T. Kouzes, and W. H. Moore, "Energy dependence of neutron sensitivity of C–$CO_2$, Mg–Ar and TE-TE ionization chambers," Phys. Med. Biol. **24**, 721–733 (1979).
[30]S. Endo, M. Hoshi, S. Suga, J. Takada, and K. Komatsu, "Determination of the relative neutron sensitivity of a C–$CO_2$ ionization chamber," Phys. Med. Biol. **41**, 1037–1043 (1996).
[31]M. Markewicz and S. Pszona, "Theoretical characteristics of a graphite ionization chamber filled with carbon dioxide," Nucl. Instrum. Methods **153**, 423–428 (1978).
[32]K. Tanaka, T. Kobayashi, G. Bengua, Y. Nakagawa, S. Endo, and M. Hoshi, "Characterization of moderator assembly dimension for accelerator boron neutron capture therapy of brain tumors using $^{7}$Li(p, n) neutrons at proton energy of 2.5 MeV," Med. Phys. **33**(6), 1688–1694 (2006).